Simple and effective models to predict the compressive and tensile strength of HPFRC as the steel fiber content and type changes

V. Savino[a], L. Lanzoni[b,c], A.M. Tarantino[c], M. Viviani[a]

[a] *HEIG-VD - Haute Ecole d'Ingénierie et de Gestion du Canton de Vaud, Route de Cheseaux 1, CH-1401 Yverdon*
[b] *DESD - Dipartimento di Economia, Scienze e Diritto, University of San Marino, Salita alla Rocca 44, Republic of San Marino, 47890 San Marino*
[c] *DIEF-Department of Engineering "Enzo Ferrari", University of Modena and Reggio Emilia, 41125 Modena, Italy*

Abstract

HPFRC/UHPC are today widely applied as repair and reinforcement materials for structures. One of the drawback of commercial HPFRC/UHPC is that the matrix mix-design changes as the proportion and type of compounds are adapted to match the market availability and to contain the costs. Any modification of the matrix mix-design affects the mechanical properties of the hardened concrete and therefore the data obtained testing the previous version of the concrete are useless. Each time the matrix changes, to unveil the relation between the matrix strengths (such as the compressive strength), the fiber volume and hardened concrete strengths (such as tensile strength), a number of new characterization tests have to be performed. Furthermore the price and performances of these materials are directly related to the fiber volume. Prediction models that link the characteristics of the fibers (shape and aspect ratio) and the matrix strengths to the performances of the hardened concrete (such as tensile, splitting and compressive strength) are of great practical interest. This paper present a simple and effective model to account for the effect of hooked or straight fibers in HPFRC as the volume of fibers changes from 0 to 5%. The model generalizes and extend the range of application of the few existing models and was successfully applied on literature data as well as on a new testing campaign. The possibility of using

Email address: luca.lanzoni@unimo.it (L. Lanzoni)

bending tests to predict the tensile strength is explored and the limits of applications of the model are presented.

Keywords: Metal-matrix composites; Mechanical properties; Numerical analysis; Mechanical testing

1. Introduction

Use of fibers to enhance the mechanical behavior of brittle materials is not a new concept. Since ancient times straw was used to reinforce sunbaked bricks, as well as horsehairs were used in masonry mortar and plaster to enhance certain mechanical properties. In 1898 the invention of the Hatschek process promoted the commercial use of asbestos fibers in a cement matrix. Between 1960 and 1970 new fiber types were introduced and substituted the asbestos fibers. In the 1960s some researchers investigated the use of steel fibers reinforcement and demonstrated the advantages of this new technology [32, 33]. With the advent of High- and Ultra high- Performance Fiber Reinforced Concrete (HPFRC/UHPFRC) the steel fibers become popular [14, 36, 35, 8, 46, 47, 52, 48, 49]. Concretes are characterized by a low tensile strength and ductility that can be improved by adding steel fibers into the matrix. Steel fibers currently used in cementitious composite materials have much evolved in the past years, thanks to a number of researches [31, 25, 19, 44, 30, 16, 39, 28, 34, 5], focusing both on the use of innovative steels and on new shapes of the fibers[1]. These new fibers further improved many engineering properties of HPFRC/UHPFRC [18, 15, 1, 26, 2] e.g. tensile strength, compressive strength, elastic modulus, crack resistance and toughness[2]. Also splitting and crushing resistance of concrete can be enhanced by using steel fibers[7][3].

[1]FRC based on synthetic fibers has been investigated, as an example, in [20, 27], whereas a recent study about the retrofitting of concrete beams strengthened by a polymer-based mortar has been addressed in [21]. The mechanical performances steel cords and a geopolymeric matrix as strengthening system has been discussed in [3].

[2]Fracture can be modelled, in a nonlinear framework, following [42], whereas recent contributes about damage mechanics can be found in [22, 23, 24]. Bifurcation and stability in the context of homogeneous finite deformations can be found in [43].

[3]An interesting study about the fibre/matrix interface in a concrete reinforced with steel fibers can be found in [38]. Experimental studies about the beneficial aspects of steel fibers in enhancing ductility of RC columns [13] and the punching shear behavior of slabs

Steel fibers are usually classified by: 1)*Geometry*: several shapes are proposed by the producers e.g. straight, hooked, undulated, flat-end etc. 2)*Equivalent diameter*: for fibers that are not circular in cross-section, the equivalent diameter is the diameter of the circle having the same area of the (average) cross-section of the actual fiber. The greater the equivalent diameter, the greater the flexural strength. 3)*Aspect ratio*: is a measure of the slenderness of the fiber defined as the ratio between the length of the fiber and the equivalent diameter (l/d_e). 4)*Volume fraction*: is the concentration of fibers within a given unit volume of composite material (V_f). 5)*Strength*: is the stress capacity that fiber reaches before failure. 6)*Toughness*: is considered as the ability of the fiber to adsorb strain energy before failure.

The performances of a HPFRC are influenced by all the above-mentioned parameters and strength of the concrete matrix. Researchers have shown that the aggregates and the steel fibers have been largely influencing both the compressive and the tensile strength of concrete (e.g. [45, 29, 41]). Literature contains a wide number of test campaigns on the mechanical properties of SFRC, HPFRC and UHPFRC but few systematic studies on the effect of the fiber volume and shape on the direct tensile strength were performed. Furthermore the preferred method to study the effect of fibers on an HPFRC/UHPFRC are splitting or bending tests that are further correlated with the ductility and other engineering properties. While many models are available for a specific dataset, few researchers attempted to construct a model that predict either the tensile, splitting or bending strength by taking into account the volume fraction of the fibers, the shape of the fibers and the matrix characteristics ([45, 29, 41] et al.). When qualifying a new HPFRC/UHPFRC for a particular field/use, the norms impose large test campaign to define the ductility and the tensile strength of the concrete ([50, 55, 56, 57]). If to this compulsory testing campaign have to be added a series of test to understand which volume and shape of fiber has to be used to meet the minimum designers requirement, then the cost of qualification might deter the use of these high technology concretes.

2. Materials and methods

For this study twenty-five combinations of steel fibers with varying shape, geometry (l/d_e) and dosage (V_f) were used. The toughness behavior was

[4] have been investigated also.

taken into account. Straight steel fibers with two different l/d_e ratios of 65, 75 and hooked-end steel fibers with three different l/d_e ratios of 45, 65 and 85 were used. For each fiber five different V_f were taken in account: 1.5%, 2%, 3%, 4% and 5%. The tensile strength of fibers ranges between 1000 and 1250 MPa. Further details are illustrated in Table 1 and Fig.1.

Code (n.)	Cube (n.)	Dog-bone (n.)	V_f (%)	l (mm)	d_e (mm)	Weigth (kg)	Strength (MPa)
Control	9	9	–	–	–	–	–
SF65	15	15	$1.5, 2, 3, 4, 5$	20	0.3	1.10×10^{-5}	1200
SF75	15	15	$1.5, 2, 3, 4, 5$	13	0.175	2.45×10^{-6}	1250
HF45	15	15	$1.5, 2, 3, 4, 5$	35	0.75	1.12×10^{-4}	1200
HF65	15	15	$1.5, 2, 3, 4, 5$	35	0.55	6.54×10^{-5}	1200
HF85	15	15	$1.5, 2, 3, 4, 5$	30	0.35	2.27×10^{-5}	1000

Table 1: Sampling parameters

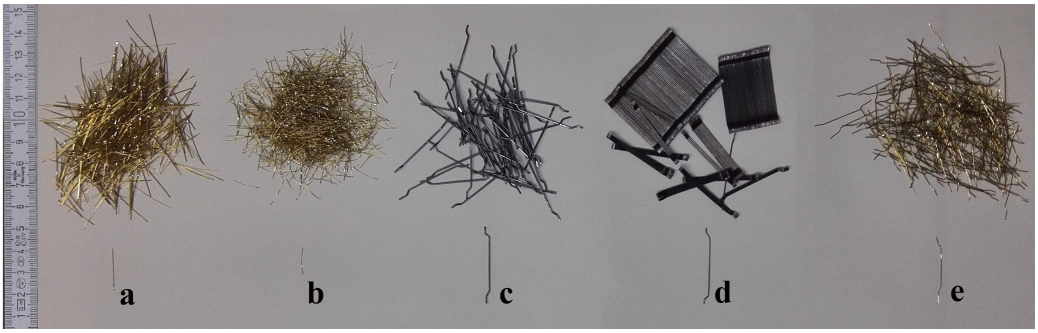

Figure 1: Types of steel fibers: a) SF65, b) SF75, c) HF45, d) HF65, and e) HF85

The exact composition of the commercial HPFRC was unknown since the producer does not provide the mix design (which is simply labeled "premix' ' and the nature of the compounds. Premixes of HPFRCs usually contain cement, sands ($<$ 2 mm) and pozzolans. To fabricate one cubic meter of HPFRC the producer prescribe the insertion in a mixer of 2226 kg of premix, 239.5 kg of water and 22.3 liters of a blend of admixtures (of unknown type, supplied with the premix). According to the producer this blend of admixtures increases the strength, enhance the durability, provide a high workability and compensate a part of the shrinkage [6]. Although fiber addiction did not modify remarkably the yield stress of the fresh mixture, they

increased the viscosity[4]. A good distribution of the fibers in the HPFRC was obtained by using a high intensity rotating pan mixer. During the casting process the lab temperature and relativity humidity were 22 ℃ and 65%, respectively. Once in the molds, concrete composite mixtures were compacted by using a vibrating table. After 24 hours the samples were demolded and cured in standard conditions until testing.

The experimental program includes twenty-five series of specimens, each one is composed by three cubes and three dog-bones samples of HPFRC reinforced with a fixed V_f of steel fibers characterized by a given l/d_e ratio and shape. For example, the specimens of the first series contain 1.5% of straight steel fibers with a l/d_e ratio of 65. Each series is labeled according to the shape, l/d_e ratio and V_f. SF and HF stand for Straight Fiber and Hooked Fiber; 65, 75, 85, etc. represents the l/d_eratio; 1.5, 2, 3, 4, 5 stand for the V_f. Moreover, a series of plain concrete samples (nine cubes and nine dog-bones) was used as control (Table 1).

Compressive strength on $100\times100\times100$ mm cubes and direct tensile strength on dog-bone specimens with 40×30 mm cross-section (Fig.2) were performed according to the relevant standards [53, 54, 55, 50, 57, 51]. The mean strength values, calculated in each series, depends on a population of three samples.

Before testing, the evaluation of both weight and density of cubes and dog-bones allowed to determine whether the shape and dimension of the molds influenced the fiber distribution and quantity in the matrix.

A compression machine Perrier type $138-5000$ kN was used to test the compressive strength of the cubes. The loading ratio was set to 0.6 MPa/sec. A W+B type LVF-200 kN machine was used to test the direct tensile strength on dog-bone specimens. The tests were carried out by controlling the axial elongation rate of the specimen that was monitored by a high precision extensometer. The deformation rate was set at 0.05 ± 0.01 mm/min. The average real time load (stress)-elongation diagram was recorded for all tensile test. The end sides of the dog-bone sample are larger than the central part, to allow the clamps of the machine to hold the specimen during test and to ensure that failure occurrs in the zone monitored by the deformation sensors (Fig.3).

[4]The mechanical interaction in time between the hosting structure and the cementitiuous reinforcemet is addressed in [9, 10, 11].

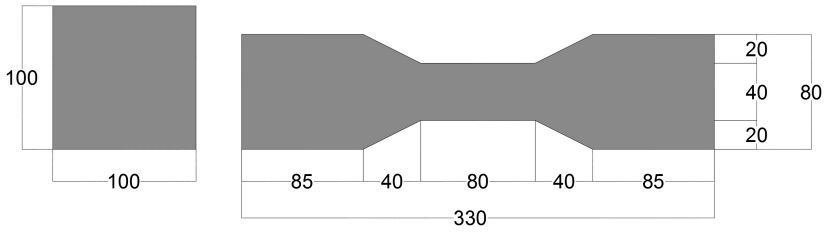

Figure 2: Sample dimensions: a) cube sample, b) dog-bone sample

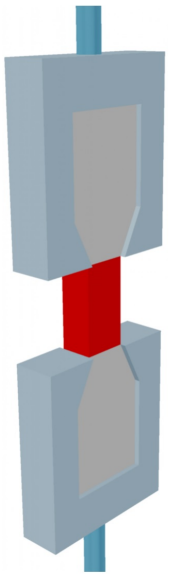

Figure 3: Zone monitored (in red) on the sample in the direct tensile test

3. Results and discussions

3.1. Fiber distribution and orientation

During the sample preparation it was observed that the workability of concrete decreased as the V_f increased. For the series HF65_5 and HF85_5 the fibers clustered together forming some fiber balls in the mixer. Thus a good distribution of fibers was not obtained and the performances of the HPFRC were compromised. Therefore the results of these series were not taken into account in this study. Workability of the fresh concrete was also influenced by the shape and l/d_e ratios of fibers. In fact SF75_5, SF65_5 and HF45_5 series did not show fiber cluster formations even if the V_f was at 5%.

Not surprisingly, steel fibers raised the specific weight of all tested concrete. It is interesting to note that the average density of dog-bone series (D) is slightly lower than cube series (C) as can be observed in Fig.4. The 4% lower specific weight is probably due to the effect of the complex geometry of the dog-bone molds (wall effect) and the filling capacity of a viscous material such as HPFRC. The orientation effects and the variability of specific weight are well-known issues, such that some standards propose to cut the dog-bones specimens from large slabs of the appropriate thickness ([50] et al.). An isotropic and homogenous distribution of fiber is also generally assumed in SFRCs. Nevertheless, the mixing, placing and vibration procedures could affect isotropy. Vibration is not strictly necessary when large quantities of HPFRC are cast, but it is advised to increase the regularity of small specimens. Several researchers [12, 40] have investigated the effect of the compaction by vibration on the orientation and segregation of fibers. Most of these investigations showed that external vibration might produce planes of preferentially oriented fibers and likely their segregation. Furthermore the torque forces exerted on the fresh concrete when is flowed are generated by shear stresses and the wall effect, two phenomena that tend to promote preferential orientations. However, in certain cases, the preferential orientation of the fibers is more interesting than isotropic distribution. If the fibers can be oriented perpendicularly to the crack planes, the toughness of the structure will be increased thanks to the higher number of fibers bridging the cracks [37]. The specific weight of each tested type of fibers (SF65, SF75, HF45, HF65 and HF85) is presented in Table 1. Specimens of the HF45 and HF65 series presented a slight fiber segregation. This could be explained considering that even if the shape of these two fibers is similar to the others they are heavier causing the segregation process.

The casting direction on the dog bone specimen tend to promote fibers orientation along the main axis due to shear stresses (arising also by the friction of the concrete with the bottom of the mold) and the wall effect. This phenomenon is virtually unavoidable since the standard dog bones have a cross section of 30×40 mm and the average length of the studied fibers is of about 30 mm. Consequently is not likely to find a randomly oriented fiber, especially oriented perpendicularly to the main axis. After testing, all samples were cut in the neighbor the failure section and the orientation was evident (Fig.5). The cubes mold were filled vertically and the fibers were aligned mainly in horizontal planes, perpendicular to the pouring direction.

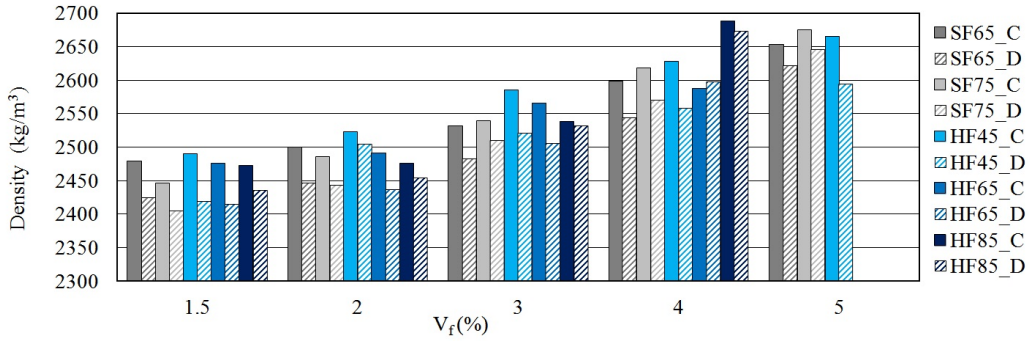

Figure 4: Comparison of the sample's density

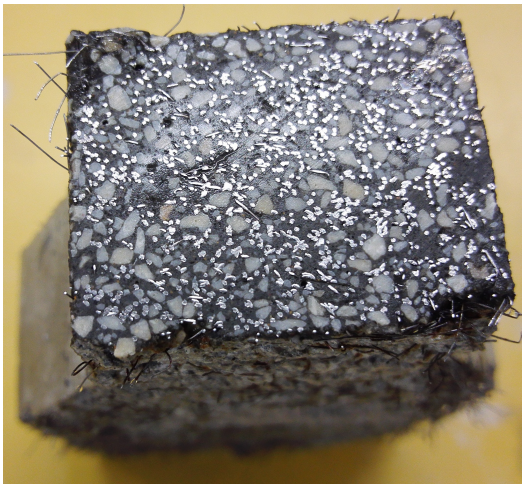

Figure 5: Distribution and orientation of steel fibers in a HPFRC dog-bone sample

3.2. Compressive strength

The compressive strength (f_c) values of HPFRC series are given in Table 2. Average compressive strength on cube specimens of the control series ($f_{c,matrix}$) was of 76 MPa. Comparing the values obtained for the control series with the concretes with fibers is evident a positive effect on the compressive strength, even if this increase is minimal for low l/d_e (about 2%) and maximum for high l/d_e ratios (about 36%), as seen in Fig.6. As V_f augments, f_c increases for all concrete series even if, at 5%, this positive effect ceased, probably due to the uneven dispersion of the fibers observed during casting operations. The small increase of f_c in concretes with hooked fibers

is probably connected with a certain degree of segregation of these heavier fibers. HF45 series shows the lowest strength increase while the HF85 series shows the greatest one. As explained in the paragraph 3.1 data for series HF65_5 and HF85_5 are not available due to impossibility of obtaining an homogenous mortar. Finally 4% of V_f seems to be the optimal rate of fibers with respect to the compressive strength and the mixing procedures.

	f_c			f_t			f_{rt}			SED	
Sample	Aver. (MPa)	COV (%)	Rel. (%)	Aver. (MPa)	COV (%)	Rel. (%)	Aver. (MPa)	COV (%)	Rel. (%)	Aver. (Mpa)	COV (%)
Matrix	75.85	9.63	100.00	3.30	9.58	100.00	–	–	–	–	–
SF65_1.5	82.17	8.57	108.33	3.73	11.27	113.03	2.41	8.70	73.03	6.99	4.48
SF65_2	83.11	5.84	109.57	5.67	12.48	171.82	2.86	24.20	86.67	7.75	27.75
SF65_3	87.53	2.48	115.40	7.08	7.51	214.55	2.26	23.94	68.48	7.37	14.68
SF65_4	100.26	1.57	132.18	7.27	14.36	220.30	1.92	30.84	58.18	7.38	13.10
SF65_5	101.35	0.81	133.62	5.07	22.41	153.64	1.85	16.43	56.06	6.31	12.07
SF75_1.5	88.56	1.26	116.76	4.17	9.90	126.36	1.13	13.16	34.24	3.78	4.63
SF75_2	89.50	2.46	118.00	4.28	20.45	129.70	0.67	35.49	20.30	3.80	34.51
SF75_3	94.44	0.19	124.51	5.10	5.43	154.55	1.47	23.13	44.55	5.86	17.30
SF75_4	97.65	2.66	128.74	6.24	5.68	189.09	0.90	23.91	27.27	4.06	4.71
SF75_5	97.74	3.05	128.86	5.91	15.61	179.09	0.83	26.99	25.15	5.36	23.56
HF45_1.5	77.47	1.07	102.14	3.41	5.03	103.33	1.65	23.06	50.00	3.07	24.36
HF45_2	78.79	5.01	103.88	3.63	1.21	110.00	1.52	6.21	46.06	4.49	10.17
HF45_3	81.25	2.19	107.12	3.77	14.36	114.24	1.42	38.26	43.03	5.49	29.09
HF45_4	83.06	2.48	109.51	4.23	29.11	128.18	1.33	22.09	40.30	5.76	6.69
HF45_5	83.70	2.96	110.35	6.87	11.73	208.18	1.80	10.27	54.55	8.41	5.66
HF65_1.5	77.52	5.67	102.20	3.74	12.75	113.33	1.21	19.36	36.67	4.39	24.95
HF65_2	81.43	2.96	107.36	3.88	11.37	117.58	1.39	32.29	42.12	6.09	13.71
HF65_3	84.66	7.07	111.62	3.89	5.00	117.88	2.36	18.81	71.52	9.69	9.00
HF65_4	89.06	7.73	117.42	5.94	8.69	180.00	2.48	1.41	75.15	9.97	6.87
HF85_1.5	81.03	6.41	106.83	4.03	5.44	122.12	1.75	30.67	53.03	6.48	12.94
HF85_2	86.15	3.07	113.58	5.43	4.47	164.55	2.75	10.05	83.33	6.79	4.21
HF85_3	96.65	0.47	127.42	5.69	12.26	172.42	2.90	12.85	87.88	7.47	11.65
HF85_4	103.52	1.44	136.48	7.34	6.34	222.42	4.17	38.88	126.36	9.05	14.20

Table 2: Results

3.3. Direct tensile strength

From direct tensile tests of each series of HPFRC three different parameters were measured or derived: tensile strength (f_t), residual tensile strength (f_{rt}) and Strain Energy Density (SED), see Fig.7. f_t is defined as the tensile tension value at the time of the first crack formation in the axial strain range of 0.01 and 0.25%. f_{rt} is the tension value corresponding to the 2% of axial strain; SED represents the area of the experimental stress-strain under graph. Each series is composed by three samples. The f_t value of the control

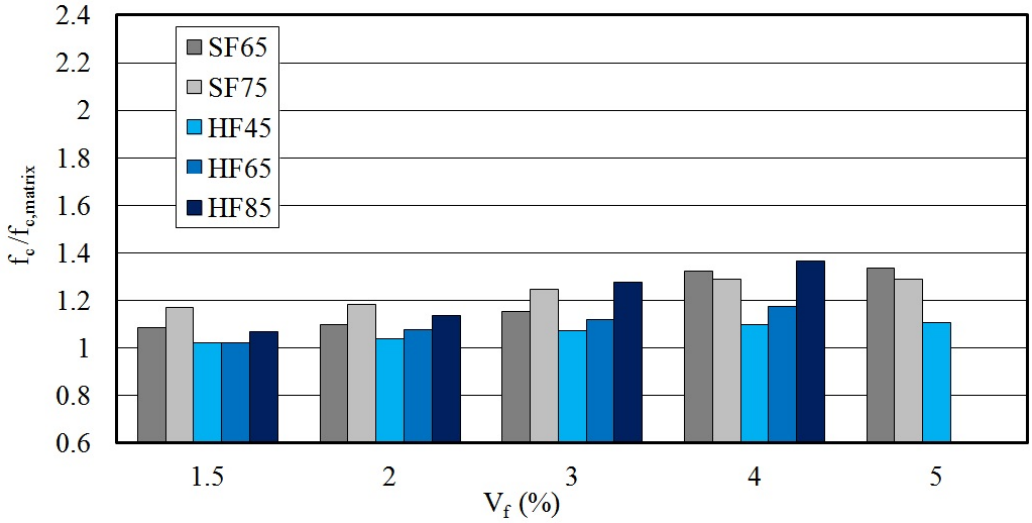

Figure 6: Effect of l/d_e ratio and V_f on f_c

series was 3.3 MPa. For series SF65, SF75, HF45, HF65, HF85 the maximum and minimum f_t values were 7.27, 6.24, 6.87, 5.94, 7.34 and 3.73, 4.17, 3.41, 3.74, 4.03 MPa, respectively. The relative strengths are presented in Fig.8 and show an increase of tensile strength in the range $3 - 122\%$ compared to the value of the control series ($f_{t,matrix}$). For all hooked fiber series, f_t increased with increasing l/d_e ratio. For SF65, SF75, HF85 series, f_t also increases with increasing V_f. In 5% series, there is a clear reduction of the peak tensile strength. Fibers were too close to develop an efficient bridging effect in the cracking section. HF45, HF65 series did not show a sensible increase of strength from 1.5% to 3% of V_f. Even though in these series some segregation occurred, for higher V_f (4 % and 5%), the distribution of the fibers in the mixture remains good and good values for the tensile strength are obtained.

A softening behavior after cracking and a not negligible residual strength until the 2% of the axial strain have been observed. Residual tensile strength (f_{rt}) values of each HPFRC series are drawn in Table 2. For series SF65, SF75, HF45, HF65, HF85 the maximum and minimum f_{rt} values were 2.86, 1.47, 1.8, 2.48, 4.17 and 1.85, 0.67, 1.33, 1.21, 1.75 MPa, respectively. The ratio between f_{rt} value of each series and $f_{t,matrix}$ ranges from 0.2 to 1.26. As shown in Fig.9, the combination SF65_2 shows the greatest f_{rt} value of all SF series, a value that drops as V_f increases. This phenomenon is also

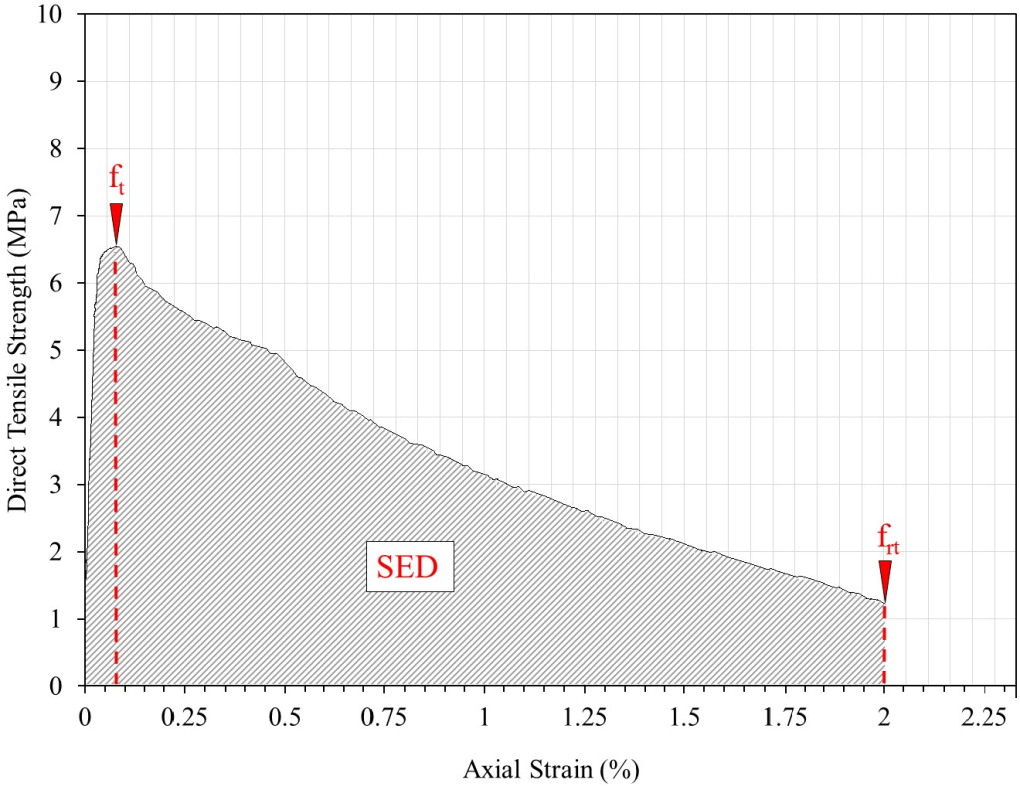

Figure 7: Parameters of the behavior of the HPFRC under direct tensile stress

observed for series SF75 whose tensile strength peak is for 3% of V_f. In the series HF45, f_{rt} decreased slightly augmenting V_f. More interesting is the behavior in HF65 and HF85 series in which f_{rt} increased with increasing V_f. In fact, thanks to both hooked-end shape and high l/d_e ratio these fibers enhance the crack bridging process improving the post-cracking behavior. The fiber bridging the cracks avoids the brittle failure of the specimens under tensile stresses and improves the toughness. Fig.10 highlights the influence of the V_f and l/d_e ratio on the toughness via the SED on each series. In SF65 series a V_f of 2% confers more ductility to the HPFRC than any other volume fraction. From that percentage onwards a slight reduction of ductility occurred while the amount of fibers increased. SF75 series showed no obvious improvement of ductility by varying the V_f. Instead hooked fiber (HF) series clearly denoted that toughness improved with the increasing of both l/d_e ratios and V_f.

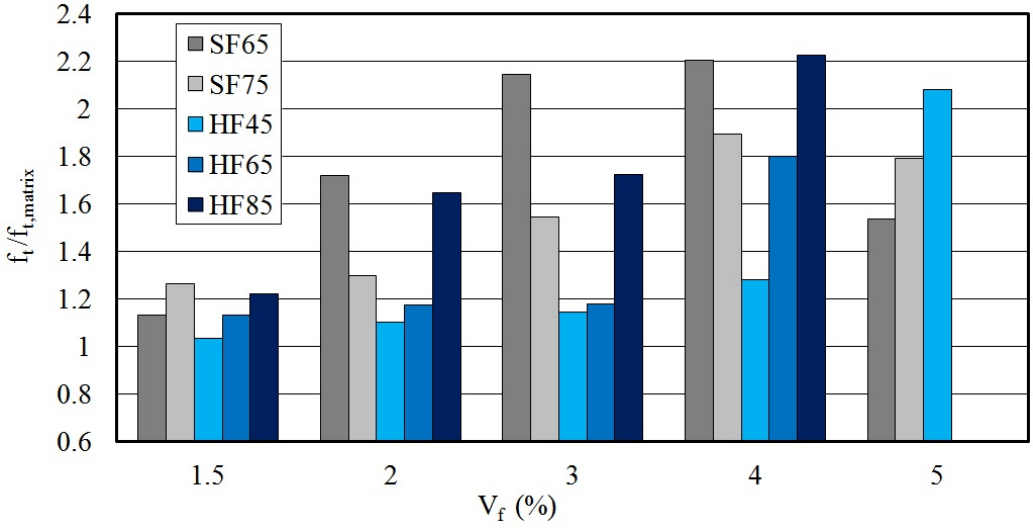

Figure 8: Effect of l/d_e ratio and V_f on f_t

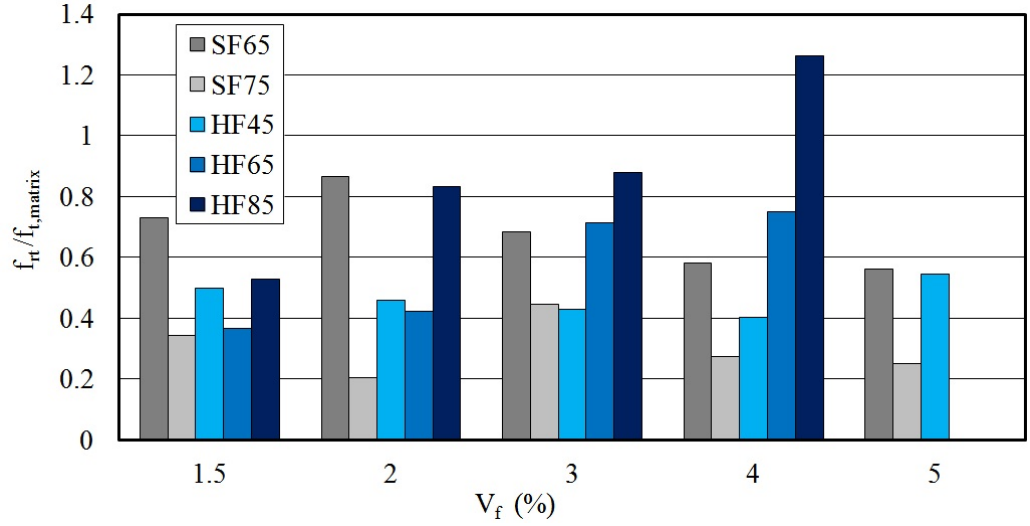

Figure 9: Effect of l/d_e ratio and V_f on f_{rt}

Before first cracking occurs all the HPFRC series tend to show a similar behavior and the tensile strength is not significantly influenced by the shape of the tested fibers (see Fig.8). After the matrix crack initiation, the stress is absorbed by the fibers bridging the cracks. On the straight fibers the deformation of the fibers will finally causes the fibers debonding and pull out.

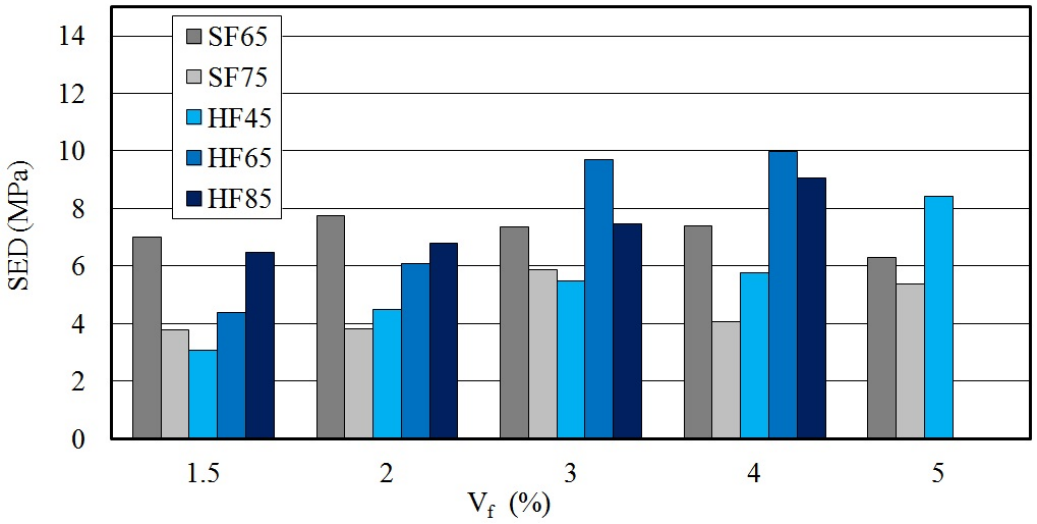

Figure 10: Effect of l/d_e ratio and V_f on SED

Instead, hooked fibers, are retained at the (hooked) ends that plasticize and further crack the surrounding matrix before the fiber is finally pulled out. In fact, the residual tensile strength is clearly higher for HPFRCs with hooked fibers. From a point of view of toughness steel fibers are well-adapted to dissipate strain energy. Even if hooked fibers offer the benefit described above the energy-absorbing capability of fibers depend also on the cross-section of fibers which encounter the crack plane and their elastic properties of the fiber. Hooked fibers are more efficient in increasing the residual tensile strength. Straight fibers conferred to the HPFRC a higher ductility for low dosages. This effect is probably due to the smaller cross section and higher number of straight fibers bridging the cracks. SF series showed higher values of ductility with V_f of 1.5 and 2%, whereas HF series overtook such as values with V_f of 3, 4 and 5%.

4. Regression models of compressive and tensile strength

4.1. Predictive models in literature

The mechanical behavior of the HPFRC is affected by the engineer properties of the reinforcing fibers, the concrete matrix and their interactions. For practical purposes is important to know how the tensile and compressive strength of a HPFRC vary when l/d_e ratio, V_f and the shape of the fibers

are changed. Such models, constructed on a specific matrix, permits to know what type and quantity of fibers have to be used in order to meet the designers' requirements.
Many predictive models have been developed. Ramadoss et al.[29] have developed a linear model to predict the compressive and tensile strength by studying the behavior of three mortars reinforced by an increasing volume of a single type of steel fibers. This model is therefore valid if the fiber features are not changed:

$$f_{cf}(\text{MPa}) = f_c + 0.0184 \times RI \tag{1}$$

$$f_{spf}(\text{MPa}) = f_{sp,matrix} + 0.006 \times RI \qquad R^2 = 0.94 \tag{2}$$

where $RI = w_f \times l/d_e, w_f =$ Density of fiber / Density of SFRC$\times V_f$.

Yazıcı et al.[45] developed a multi-linear relationship between the strength (tensile and compressive) of a HPC concrete, l/d_e ratio and V_f. In this case one matrix was investigated with three types of steel (hooked) fibers:

$$f_{cf}(\text{MPa}) = 50.4869 + 0.0434 \times l/d_e + 1.9667 \times V_f(\%) \qquad R^2 = 0.10 \tag{3}$$

$$f_{spf}(\text{MPa}) = 2.2121 + 0.0077 \times l/d_e + 1.4233 \times V_f(\%) \qquad R^2 = 0.72 \tag{4}$$

Sumathi et al.[41] used a second order polynomial equation to regress the relationships between the strength of the composite concrete and V_f while l/d_e ratio is kept constant. Also in this investigation the fibers were hooked:

$$f_{cf}(\text{MPa}) = 41.45 + 9.984 \times V_f - 3.837 \times V_f^2 \qquad R^2 = 0.91 \tag{5}$$

$$f_{spf}(\text{MPa}) = 3.925 + 1.448 \times V_f - 0.042 \times V_f^2 \qquad R^2 = 0.99 \tag{6}$$

where f_c, f_{cf}, $f_{sp,matrix}$, f_{spf} and RI are the mean compressive strength of the matrix mortar, mean compressive strength of the fibrous concrete, mean splitting tensile strength of the matrix mortar, mean splitting tensile strength of the fibrous concrete and reinforcing index, respectively.

4.2. Validation of a general model

The above presented models (equations 1-6) were used on the testing campaign described in the section 2. Furthermore they were applied also to data obtained with straight fibers. Finally a new and more general model was developed and compared with the existing literature.
The new model aims to predict f_c, f_t and f_{rt} of a HPC reinforced by steel

fibers with different shapes, l/d_e ratios and V_f ranging from 0 to 5%.
Experimental relationships between fiber parameters (such as l/d_e ratio and V_f) and f_c, f_t and f_{rt} have been established by using a multiple linear regression analysis with a confidence of 95% (equations 7,8,9), as seen in [45]. This model showed the highest R^2 values of all models taken into consideration. If for straight fibers a new model proved to be useful, the behavior of the concrete reinforced by hooked fiber is well predicted by using a linear model according to [29] (equations 10,11,12).

$$f_{cSF}(\text{MPa}) = 75.0663 + 0.0499 \times l/d_e + 4.4344 \times V_f(\%) \quad R^2 = 0.83 \quad (7)$$

$$f_{tSF}(\text{MPa}) = 3.5333 + 0.0029 \times l/d_e + 0.5452 \times V_f(\%) \quad R^2 = 0.34 \quad (8)$$

$$f_{rtSF}(\text{MPa}) = 10.8829 - 0.1260 \times l/d_e - 0.1396 \times V_f(\%) \quad R^2 = 0.81 \quad (9)$$

$$f_{cHF}(\text{MPa}) = f_{c,matrix} + 0.0185 \times RI \quad R^2 = 0.76 \quad (10)$$

$$f_{tHF}(\text{MPa}) = f_{t,matrix} + 0.003 \times RI \quad R^2 = 0.68 \quad (11)$$

$$f_{rtHF}(\text{MPa}) = 0.4992 + 0.0028 \times RI \quad R^2 = 0.68 \quad (12)$$

In Figs.11, 12, 13 the models of the author and the test results are plotted. It can be immediately observed the different behavior between the HPC reinforced with straight fibers and that reinforced with with hooked fibers. Both compressive and tensile strength values of the concrete reinforced by straight fibers are higher for low to medium fibers dosages (up to 2%). For higher dosages (from 3%) the hooked fibers show the best performances, especially in term of residual tensile strength (Fig.13). This is also the reason why many researchers have concentrated their effort on hooked fibers.

Fig.14, 15 and 16 show the relationships between calculated and predicted strength values (see equations 7-12) for all types of fibers. The coefficients of correlation (R^2) between calculated and predicted values are 0.87, 0.47, 0.85, 0.83, 0.77, and 0.77 for f_{cSF}, f_{tSF}, f_{rtSF}, f_{cHF}, f_{tHF} and f_{rtHF}, respectively. The high R^2 values confirm that the shape, l/d_e ratio and V_f play an important role in improving the compressive and direct tensile strength of HPFRCs. Furthermore, the strength is proved to be deeply influenced by the fiber parameters. It is interesting to note that f_{rt} of a concrete reinforced by straight fiber does not increase when l/d_e ratio and V_f fraction increase. Instead, for concrete reinforced with hooked fibers, f_{rt} improves with increasing l/d_e ratio and V_f (see Fig.13).
In Fig.17a the new models used for HPCs reinforced by steel hooked fibers (according to equations 10, 11, 12) are plotted and compared with the literature (see 4.1). Most of the models found in literature have been developed by

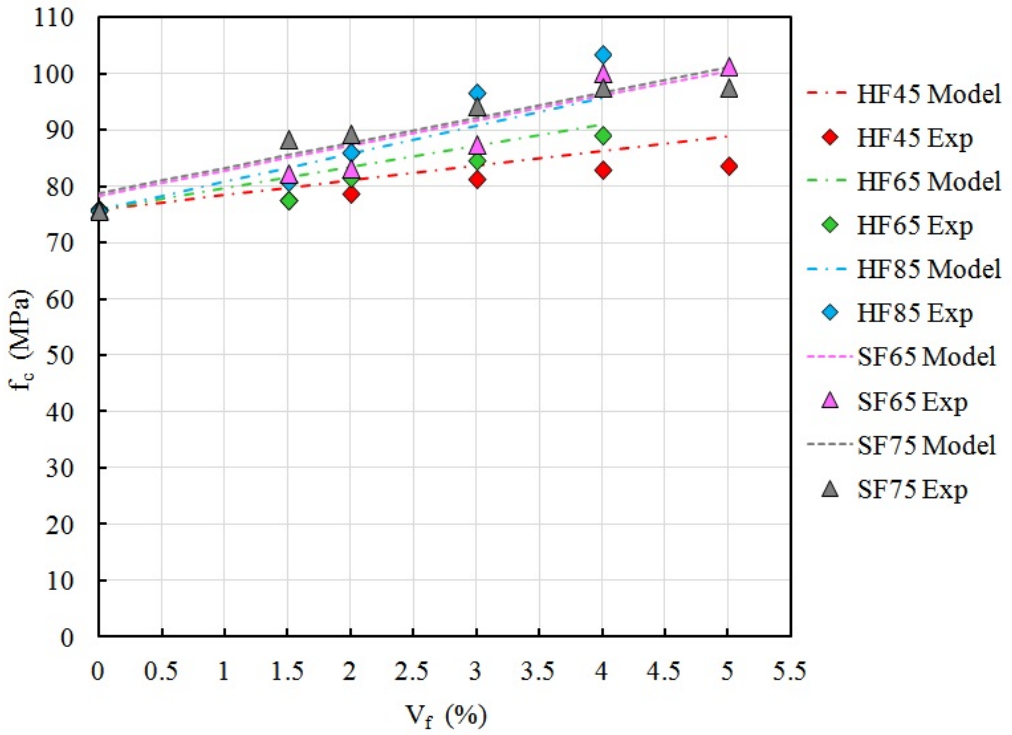

Figure 11: Models of compressive strength

studying a limited range of l/d_e ratios and V_f and therefore it was necessary to extend them beyond of the experimental evidences. The dotted lines in the Fig.17 and Fig.18 are the range of values obtained extending the prediction of the equations 1-6, permitting a comparison with the author's models and tests (in this research the V_f up to 5% was used). It can be observed that all compressive strength models have a similar slope and confirms that the strength of the HPFRC increases when l/d_e ratio and V_f increase. [29] have taken into account the strength of the matrix as variable of the model i.e. for a $V_f = 0$; $f_c = f_{c,matrix}$. The compressive strength of the matrix of the SFRCs investigated in [45] and [41] is not a variable but corresponding approximately to the y-intercept parameter of the model carried out from the equation 3 ($\sim$ 50 MPa) and equation 5 ($\sim$ 40 MPa), respectively. Substituting the y-intercept value of the equation 3 with the matrix strength value investigated by the author it observes that also the model in [45] well

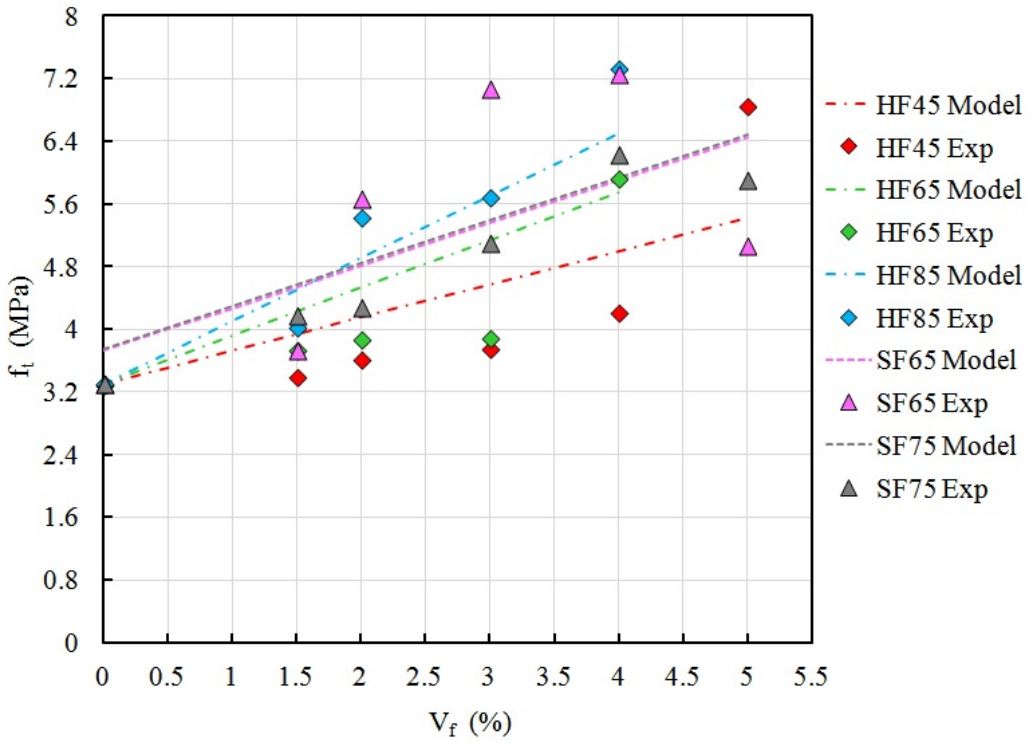

Figure 12: Models of tensile strength

agrees with both the model of the author and [29] (Fig.17b). This assumption highlights that the matrix performances strongly condition the magnitude of the effect of the fibers on the strength of the HPFRC and that similar fibers lead to similar prediction on the strength gain for similar volumes of fibers. The value of the compressive strength of the matrix investigated in this work is also substituted in the model of [41] as the y-intercept parameter in the equation 5. In this case, as shown in Fig.17b, the compressive strength of the SFRC increases until the fiber dosage does not exceed 1.5 %; for higher dosages, the compressive strength decreases. The poor prediction in the model of [41] is likely due to the low strength of the matrix investigated that was not a HPC. Concluding, the model of the author has a good agreement with the models of [45] and [29] for the compressive strength of a HPFRC, if the strength of the matrix is taken into account in the model as variable and if the compressive strength of the matrix is higher than 50 MPa. These

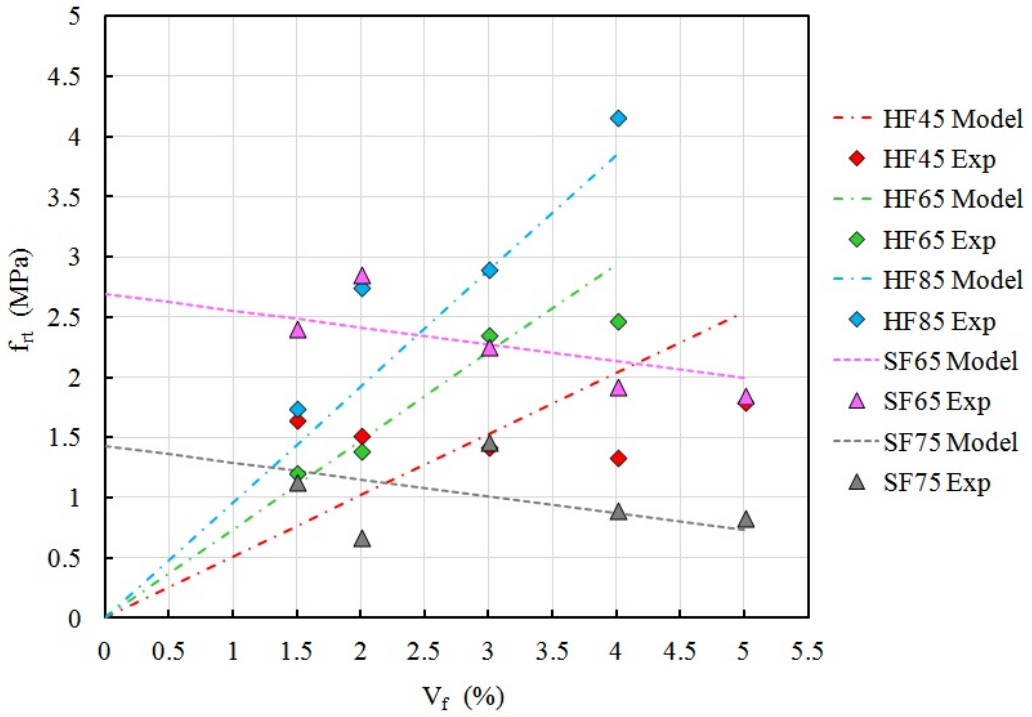

Figure 13: Models of residual tensile strength

models proved to be valid up to V_f of 5% and for l/d_e ratios ranging from 45 to 85 (see Fig.17b). In Fig. 17, A,R,Y and S stand respectively for: the model of the author, [29], [45] and [41].

Tensile strength can be measured either by indirect methods such as the splitting test (ST) or by direct test (DT) methods. The models found in literature to predict the tensile strength have been developed mainly by ST (equations 2, 4, 6), due to the fact that fluctuations of the experimental results are lower and the R^2 values are higher than the results obtained by DT methods. In this work a DT method was used to construct a prediction model. The new prediction model shows good R^2 values (see equations 7-12). The relation between tensile strength tested by ST and DT has been studied by many authors [17], and the CEB-FIP 90 model defines a relationship between the DT and ST tensile strength as follows:

$$f_{ct,dt} = 0.9 \times f_{ct,st} \tag{13}$$

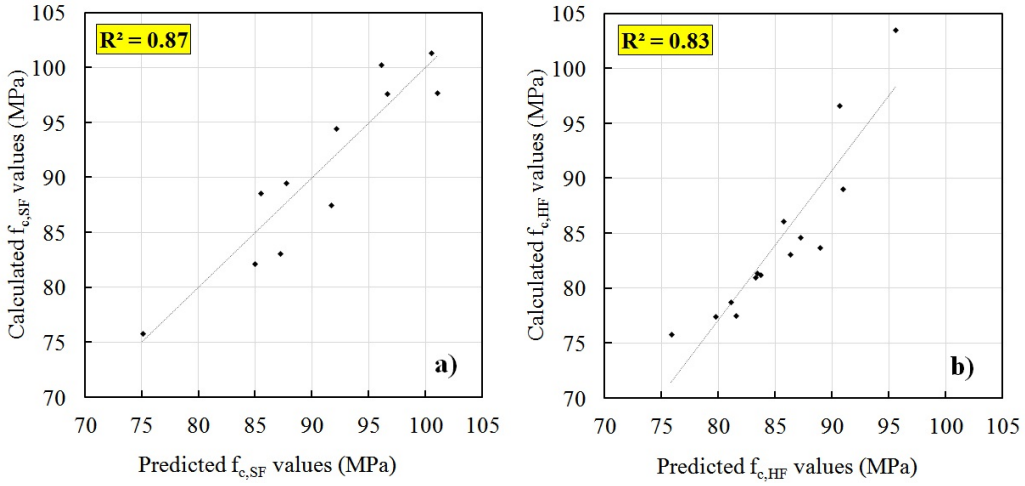

Figure 14: a) Correlation between calculated and predicted $f_{c,SF}$ values, b) Correlation between calculated and predicted $f_{c,HF}$ values

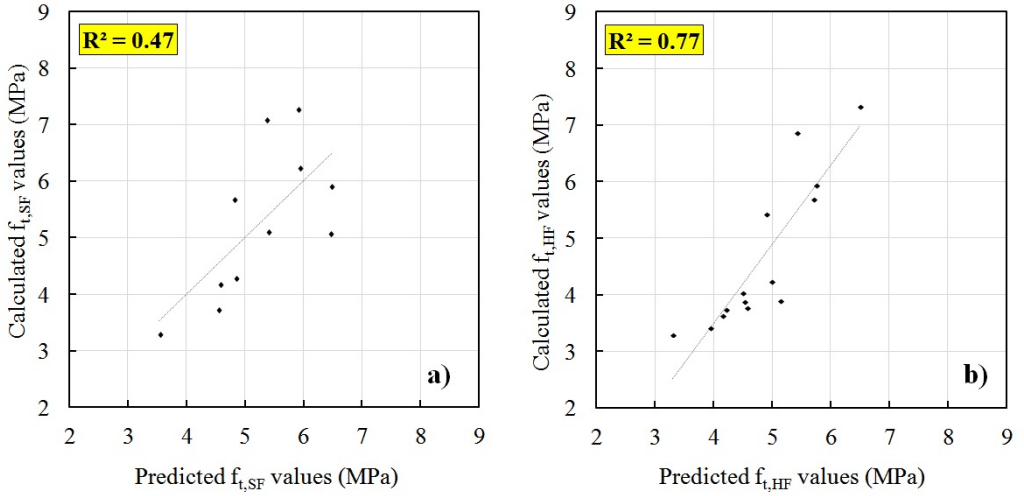

Figure 15: a) Correlation between calculated and predicted $f_{t,SF}$ values, b) Correlation between calculated and predicted $f_{t,HF}$ values

where $f_{ct,dt}$ is the mean direct tensile strength and $f_{ct,st}$ is the mean splitting tensile strength. Equation 13 was applied in the equations 2, 4, 6 and results are compared with the model of the author described in the equation 11. $f_{t,matrix}$ of the HPC investigated by [29] is a variable of the model (see equation 2). In the models of [45] (see equation 4), and [41] (see equation 6),

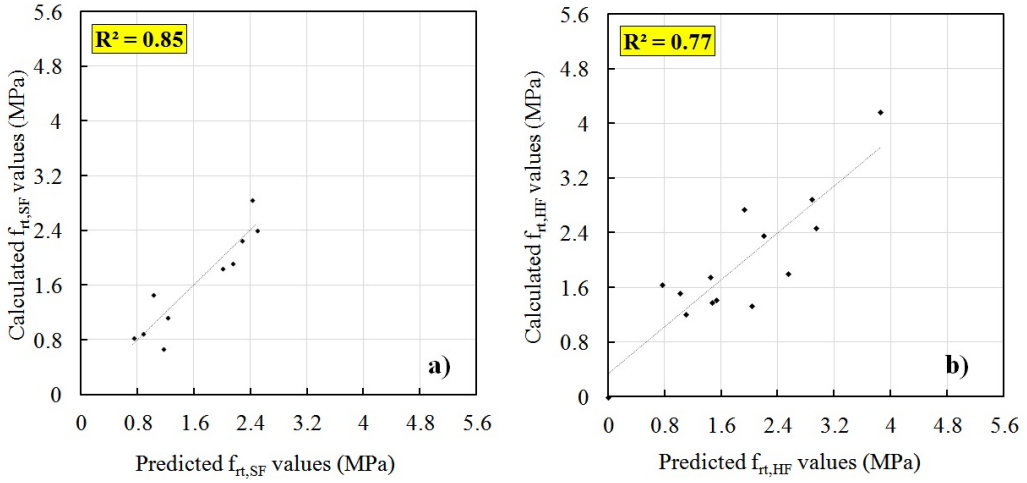

Figure 16: a) Correlation between calculated and predicted $f_{rt,SF}$ values, b) Correlation between calculated and predicted $f_{rt,HF}$ values

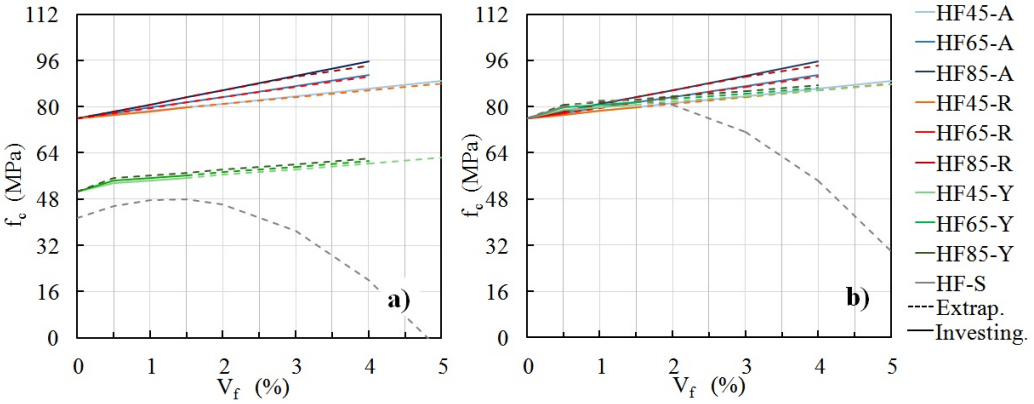

Figure 17: a) Models of compressive strength, b) Models whose y-intercept value corresponds to the $f_{c,matrix}$ of the HPFRC investigated by the author

$f_{t,matrix}$ values are fix values (4.06 and 4.00 MPa, respectively). Therefore these two models were modified by using the $f_{t,matrix}$ ($V_f = 0$) of the HPC investigated by the author (3.3 MPa) in equation 4 and equation 6. The comparison between the corrected models is showed in Fig.18a. The divergence between results increases as l/d_e ratio and V_f increase.

To further improve the models another formulation to convert the ST strength in DT strength was used. From equation 2 and 11 it can be observed that the slope-intercept of equation 2 is two times the one of equation 11. There-

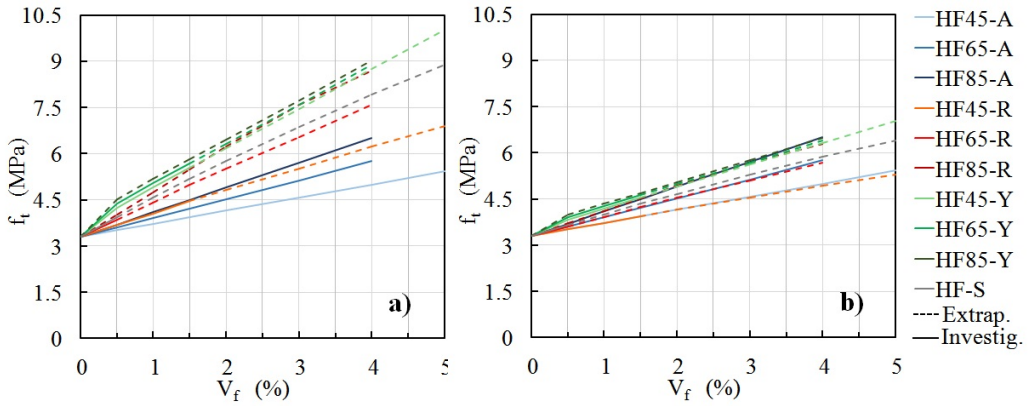

Figure 18: a) Models of tensile strength by using equation 13; b) Models of tensile strength by using equation 14

fore, assuming that the ratio value between $f_{sp,matrix}$ ($V_f = 0$) and $f_{t,matrix}$ ($V_f = 0$) is two, it might be written:

$$f_{ct,dt} = 0.5 \times f_{ct,st} \tag{14}$$

Fig.18 b shows the comparison between the models by using equation 14 for $f_{ct,dt}$ and the author's value for $f_{t,matrix}$ ($V_f = 0$). After these two corrections the four models yield very close results. Furthermore the model of the author extends the prediction of strength of a HPFRC up to V_f of 5 % and for l/d_e ratios ranging from 45 to 85.

5. Conclusions

An investigation on the influence of steel fiber properties on the compressive strength, tensile strength and toughness of a commercial HPFRC was conducted. As expected the analysis of the results demonstrate that the mechanical behavior of the tested HPFRC is influenced by the shape of fibers, aspect ratio and volume fraction. A new linear mathematical relationships could be established and applied to the new and the literature dataset. The following conclusions are drawn.

A series of linear relationships between the fibers parameters such as l/d_e ratio and V_f and the strength (compressive and tensile) of a HPFRC could be established. These relationships, established both for hooked and straight

fibers, extend the range of application of the models found in literature to determine the optimal dosage, shape and aspect ratio of fibers that will allow to meet the designers requirements in term of compressive, direct tensile and residual tensile strength of a given HPFRC.
The work confirms that a limited number of tests might be appropriate for quality control purposes, thus reducing the overall cost of the HPFRCs.
One of the main variable of all the models is the matrix strength; for ordinary concrete (compressive strength lower than 50 MPa) these relationships cannot be used.
The specific weight of the investigated HPFRC increases with using steel fibers until the soil of 300 kg/m^3 is reached.
The compressive and tensile strength increase between $2-36\%$ and $3-122\%$, respectively when fibers are added to the plain HPC. This result shows the efficiency of both straight and especially hooked steel fibers.
The use of steel fibers influences considerably the toughness of the concrete, when the dosage increases both in high (85) and low (45) aspect ratio cases a limited improvement in ductility and workability as well occurred.
The mixing, casting and vibration procedures influence the distribution, orientation and segregation of fibers. As a consequence, some cases of segregation and fiber cluster (balls) formation were observed. For these mixes a loss of both strength and toughness at the hardened state occurred.
Finally, this investigation permitted to establish that, if the matrix characteristics of a commercial product are not changed or the changes are limited, than a limited testing campaign might be sufficient to predict the behavior of the new material.

Acknowledgments

Authors gratefully acknowledge the financial support provided by HEIG-VD. Financial support from the Italian Ministry of Education, University and Research (MIUR) in the framework of the Project PRIN "COAN 5.50.16.01" - code 2015JW9NJT - is gratefully acknowledged.

References

[1] Ahlborn, T.M., Puese, E.J., Misson, D.L. *Ultra-High Performance Concrete for Michigan Bridges*. Material Performance-Phase I,MDOT RC-1525CSD-2008-11, pp. 190

[2] Bastien-Masse, M., Brühwiler E. *Concrete bridge deck slabs strengthened with UHPFRC.* IABSE Conference Rotterdam Assessment, Upgrading and Refurbishment of infrastructures, 2013, 99, pp. 236 − 237

[3] Bencardino, F., Condello, A., Ashour, A.F. *Single-lap shear bond tests on Steel Reinforced Geopolymeric Matrix-concrete joints.* Composites Part B, 110, 2017, 62–71.

[4] Caratelli, A., Imperatore, S., Meda, A., Rinaldi, Z. *Punching shear behavior of lightweightfiber reinforced concrete slabs.* Composites Part B, 99, 2016, 257–265.

[5] Won-Chang Choi, Seok-Joon J., Hyun-Do Y. *Bond and cracking behavior of lap-spliced reinforcing bars embedded in hybrid fiber reinforced strain-hardening cementitious composite (SHCC).* Composites Part B, 108, 2017, 35–44

[6] Collepardi M. *Chemical admixtures today* Proceedings of Second International Symposium on Concrete Tecnology for Sustainable February - Development with Emphasis on Infrastructure, Hyderabad, India, 27 February 3 March (2005) pp. 527 − 541.

[7] Conforti, A., Tiberti, G., Plizzari, G.A. *Splitting and crushing failure in FRC elements subjected to a high concentrated load.* Composites Part B, 105, 2016, 82–92.

[8] Daniel, J. I., Shah, S. P. *Thin-Section Fiber Reinforced Concrete and Ferrocement.* SP-124, American Concrete Institute, Detroit, 1990, 441 pp.

[9] Dezi L, Tarantino AM. *Time dependent analysis of concrete structures with variable structural system.* ACI Materials Journal, 88(3), 1991, 320-324.

[10] Dezi L, Menditto G, Tarantino AM. *Homogeneous structures subjected to successive structural system changes* - ASCE Journal of Engineering Mechanics, 116(8), 1990, 1723-1732.

[11] Dezi L, Menditto G, Tarantino AM. *Viscoelastic heterogeneous structures with variable structural system* - ASCE Journal of Engineering Mechanics, 119(2), 1993, pp. 238-250

[12] Edgington, J., Hannant, D.J. *Steel fibre reinforced concrete. The effect on fibre orientation of compaction by vibration*. Materials and Structures 5 (25) (1972) pp. 41 − 44.

[13] Germano, F., Tiberti G., Plizzari, G. *Experimental behavior of SFRC columns under uniaxial and biaxial cyclic loads*. Composites Part B, 85 (2016) 76–92

[14] Gesoglu, M., Gneyisi, E., Muhyaddin, G.F., Asaad, D.S. *Strain hardening ultra-high performancefiber reinforced cementitious composites: Effect offiber type and concentration*. Composites Part B 103, 2016, 74–83

[15] Hannawi, K., Bian, H., Prince-Agbodjan, W., Raghavan, B. *Effect of different types offibers on the microstructure and the mechanical behavior of Ultra-High Performance Fiber-Reinforced Concretes*. Composites Part B 86, 2016, 215–220

[16] Jiang L, Niu, D.T., Bai, M. *Experiment Study on the Frost Resistance of Steel Fiber Reinforced Concrete*. Advanced Materials Research, 2010, 243, pp. 150 − 151

[17] Kang S., Park J., Ryu G., Koh G., Kim S. *Comparison of Tensile Strengths with Different Test Methods in Ultra High Strength Steel-Fiber Reinforced Concrete (UHS-SFRC)*. Trans Tech Publications, 417 − 418, 2010, pp. 649 − 652

[18] Lackey, T., Desgagne, G., Benmokrane, B., El-Salakawy. E., El-Ragaby, A. *Construction and monitoring of four innovative concrete bridge decks using non-corrosive FRP composite bars*. Annual Conference of the Transportation Association of Canada, 2004, pp. 1 − 20

[19] Lane, R., Craig, B., Babcock, W. *Materials for Blast and Penetration Resistance*. Materials Ease The AMPTIAC Quarterly, Vol. 6, No. 4, 2002.

[20] Lanzoni L, Nobili A, Tarantino AM. *Performance evaluation of a polypropylene-based draw-wired fibre for concrete structures*. Construct. Build. Mater. 28 (2012) 798-806.

[21] Lanzoni L, Soragni M, Tarantino AM, Viviani M. *Concrete beams stiffened by polymer-based mortar layers: Experimental investigation and modeling*. Construction and Building Materials 105 (2016) 321-335.

[22] Lanzoni L, Tarantino AM. *Damaged hyperelastic membranes*. Int. J. NonLinear Mech. 60 (2014) 9–22.

[23] Lanzoni L, Tarantino AM. *Equilibrium configurations and stability of a damaged body under uniaxial tractions*. ZAMP Zeitsc. Angew. Math. Phys. 66(1) (2015) 171–190.

[24] Lanzoni L, Tarantino AM. *A simple nonlinear model to simulate the localized necking and neck propagation*. Int. J. NonLinear Mech. 84 (2016) 94-104.

[25] Moser, R.D. *High-Strength Stainless Steels for Corrosion Mitigation in Prestressed Concrete: Development and Evaluation*. Ph.D. Dissertation, Georgia Institute of Technology, Atlanta, GA, 2011

[26] Nazar, S., Ismaiel, M.A., Ahmed, M. *Possibility to Improve Strength and Structural Stability of Bridge Deck Slabs by Using Ultra High Performance Fiber Reinforced Concrete*. IOSR J Mechanical and Civil Engineering, 2014;11, pp. $79 - 87$

[27] Nobili A, Lanzoni L, Tarantino AM. *Experimental investigation and monitoring of a polypropylene-based fiber reinforced concrete road pavement*. Construct. Build. Mater. 47 (2013) 888-895.

[28] Popa, M., Corbu, O., Kiss, Z., Zagon, R. *Achieving Mixtures of Ultra-High Performance Concrete*. ConstructII 2013; 1, pp. $40 - 46$

[29] Ramadoss P., Nagamani K. *Tensile strength and durability characteristics of high-performance fiber reinforced concrete* . The Arabian Journal for Science and Engineering, 33, $2B$, 2008, pp.$307 - 319$

[30] Ramli M, Dawood, E. *High-Strength Flowable Mortar Reinforced by Steel Fiber*. Slovak Journal of Civil Engineering 2011, 19(3), pp. $10 - 16$

[31] Rivera-Soto, P., Moser, R.D., McClelland, Z.B., Williams, B.A., Williams, S.L. *Thermal Processing and Alloys Selection to Modify Steel Fiber Performance in Ultra-High Performance Concrete*. First International Interactive Symposium on UHPC, 2016

[32] Romualdi, J. P., Batson, G.B. *Mechanics of Crack Arrest in Concrete*. Journal of the Engineering Mechanics Division., ASCE, Vol. 89, No. EM3, June 1963, pp. 147-168.

[33] Romualdi, J. P., Mandel, J. A. *Tensile strength of concrete affected by uniformly distributed closely spaced short lengths of wire reinforcement.* American Concrete Institute, K. Proc., 61(6), 1964, pp. 657 − 671

[34] Sanal, I., Ozyurt, N., Hosseini, A. *Characterization of hardened state behavior of self compactingfiberreinforced cementitious composites (SC-FRCC's) with different beam sizes andfiber types.* Composites Part B, 105, (2016) 30–45.

[35] Shah, S. P., Batson, G. B. *Fiber Reinforced Concrete Properties and Applications.* SP-105, American Concrete Institute, Detroit, 1987, 597 pp.

[36] Shah, S. P., Skarendahl, A. *Steel Fiber Concrete.* Elsevier Applied Science Publishers, Ltd., 1986, 520 pp.

[37] Shah, Surendra, P., Brandt, A.M., Ouyang, C., Baggot, R., Eibl, J., Glinicki, M.A., Krenchel, H., Lambrechts, A., Li, V.C., Mobasher, B., and Taerwe, L. *High Performance fibre reinforced cement composites* . High Performance Fiber Reinforced Cement Composites 2. Chapter 6 2 1996.

[38] Sim oes, T., Octavio, C., Valena, J., Costa, H., Dias-da-Costa, D., Jlio, E. *Influence of concrete strength and steelfibre geometry on the fibre/matrix interface.* Composites Part B 122 (2017) 156–164

[39] Slater, E., Moni, M., Alam, M.S. *Predicting the shear strength of steel fiber reinforced concrete beams.* Construction and Building Materials, 2012, 26, pp. 423 − 436

[40] Stroeven, P. *Morphometry of fibre reinforced cementitious materials, Part II: Inhomogeneity, segregation and anisometry of partially oriented fibre structures.* Materials and Structures 12 (1979) pp. 9 − 20.

[41] Sumathi A., Saravana Raja Mohan K. *Study on the Strength and Durability Characteristics of High Strength Concrete with Steel Fibers* . International Journal of ChemTech Research, 8, 1, 2015, pp. 241 − 248

[42] Tarantino AM. *Nonlinear fracture mechanics for an elastic Bell material.* Quart. J. of Mech. and Appl. Math. 50(3), 1997, 435-456.

[43] Tarantino AM. *Homogeneous equilibrium configurations of a hyperelastic compressible cube under equitriaxial dead-load tractions* - Journal of Elasticity, 92, 2008, pp. 227-254.

[44] Tjahjanto, D.D., Suiker, A.S.J., Turteltaub, S., Rivera Diaz del Castillo, P.E.J., van der Zwaag, S. *Micromechanical predictions of TRIP steel behavior as a function of microstructural parameters*. Computational Materials Science, Vol. 41, 2007, pp. 107 − 116

[45] Yazıcı Ş, İnan G, Tabak V. *Effect of aspect ratio and volume fraction of steel fiber on the mechanical properties of SFRC*. Construction Building Material 2007;21:12503. doi:10.1016/j.conbuildmat.2006.05.025

[46] Yoo, D.Y., Banthia, N., Yoon, Y.S. *Predicting service deflection of ultra-high-performancefiberreinforced concrete beams reinforced with GFRP bars*. Composites Part B, 99 (2016) 381–397

[47] ACI Committee 544 *Revision of State-of-the-Art Report (ACI 544 TR-73) on Fiber Reinforced Concrete*. American Concrete Institute JOURNAL, Proceedings, Nov. 1973, Vol. 70, No. 11, pp. 727 − 744.

[48] ACI Committee 544 *State-of-the-Art Report (ACI 544 1R-82(86)) on Fiber Reinforced Concrete*. American Concrete Institute JOURNAL, 1982, Detroit, MI, 22 pp.

[49] ACI Committee 506 *State-of-the-Art Report (ACI 506 1R-84(89)) on Fiber Reinforced Shot-crete*. American Concrete Institute JOURNAL, Detroit, MI, 13 pp.

[50] CNR-DT 204 *Guidelines for design, construction and production control of fiber reinforced concrete structures*. National Research Council of Italy, 2006

[51] PrSIA 2052 *Béton fibré ultra-performant (BFUP)-Matériaux, dimensionnement et exécution* 2015-05

[52] RILEM Technical Committee 19-FRC *Fibre Concrete Materials*. Materials and Structures, Test Tes., Vol. 10, No. 56, 1977, pp. 103 − 120.

[53] UNI EN 206-1 *Concrete Part 1: Specification, performance, production and conformity*. 2006

[54] UNI EN 12390-3 *Testing hardened concrete Compressive strength of test specimens*. 2003

[55] UNI 11039-1 *Steel fibre reinforced concrete Definitions, classification and designation.* 2003

[56] UNI 11039-2 *Steel fibre reinforced concrete Test method for determination of first crack strength and ductility indexes* 2003

[57] UNI 11188 *Steel fibres reinforced concrete structural elements Design, execution and control.* 2007

List of Figures